EUSIPCO 2013 1569743551

NUMERICAL PERFORMANCE OF A TENSOR MUSIC ALGORITHM BASED ON HOSVD FOR A MIXTURE OF POLARIZED SOURCES

Maxime Boizard[12], *Guillaume Ginolhac*[13], *Frédéric Pascal*[2], *Sebastian Miron*[4], *Philippe Forster*[1]

[1] Laboratoire SATIE - ENS Cachan - CNRS - UniverSud, France
[2] Laboratoire SONDRA - Supelec, France
[3] LISTIC - Université de Savoie, France
[4] CRAN - Université de Lorraine, France

ABSTRACT

In this paper, we develop an improved tensor MUSIC algorithm adapted to multidimensional data by means of multilinear algebra tools. This approach allows to preserve the multidimensional structure as the signal and the noise subspaces are estimated from the Higher Order Singular Value Decomposition (HOSVD) of the covariance tensor. The proposed algorithm is applied to a polarized source model. By computing the Mean Squared Error (MSE) for different scenarios, the performance of this method is compared to the classical MUSIC algorithm as well as the vector MUSIC algorithm that includes the polarization information. The simulations show that our algorithm outperforms the vector algorithms.

Index Terms— Tensor MUSIC, HOSVD, DOA Polarimetric sources estimation

1. INTRODUCTION

An increasing number of signal processing applications deal with multidimensional data like polarimetric STAP [1], polarized seismic sources localization [2], multidimensional harmonic retrieval [3, 4] or MIMO coding [5]. The multilinear algebra [6, 7] provides a good framework to exploit these data [8, 9, 3] by conserving the multidimensional structure of the information. Nevertheless, generalizing matrix-based algorithms to the multilinear algebra framework is not a trivial task. In particular, there is no multilinear extension of the Singular Value Decomposition (SVD), having exactly the same properties as the SVD. However, two main decompositions exist: CANDECOMP/PARAFAC (CP) [10, 8, 9], which conserves the rank properties of SVD and the identifiability properties, and the Higher Order Singular Value Decomposition (HOSVD) [7], which keeps the orthogonality properties.

This paper focuses on the problem of polarized source parameters estimation (Direction Of Arrival (DOA) and polarization parameters) by using a novel version of the well-known MUltiple SIgnal Classification (MUSIC) algorithm adapted to multidimensional configurations. Classically the data received on an array correspond to a vector whose dimension is equal to the number of sensors. If an additional dimension is available (e.g. polarization, emitters sensors for a MIMO configuration, Doppler frequency etc…), the data turns out to be multidimensional. Then two approaches are possible. Firstly, the *vector* approach consists in unfolding the data into vectors and applying the traditional MUSIC algorithm. The *tensor* approach, conserves the multidimensional structure of the recorded data by computing a data covariance tensor. This implies to choose a tensor decomposition in order to estimate the signal and noise subspaces.

There are several previous works on multidimensional MUSIC. A MUSIC algorithm for electromagnetic vector-sensor array is derived in [11] for the case of correlated sources.. The algorithm relies on a covariance tensor approach but its purpose is the joint use of spatial and polarimetric smoothing in order to solve the correlation issue. Moreover this method does not use a tensor decomposition and is not appropriate for our problem since we considered the case of uncorrelated sources. A DOA estimation algorithm using a tensorial approach based on CP has also been introduced in [12]. This algorithm estimates the DOA directly without estimating the signal and noise subspaces. It is applied to the same model as in [11]. Nevertheless, the iterative Alternating Least Squares squares procedure, used for fitting the PARAFAC model may exhibit convergence problems in some cases. Furthermore, depending on the data, the identifiability is not always guaranteed, making impossible the use of this algorithm. An another tensor MUSIC algorithm, Long Vector MUSIC (LVMUSIC), is proposed in [2]. However this algorithm does not fully exploit the multidimensional structure of the covariance tensor and therefore it is equivalent to the vector approach.

In this paper, we work on the model of [2]. We derive a tensor MUSIC algorithm which take account of the multidimensional data structure without the potential problems of CP. Due to its orthogonality properties, the HOSVD seems to be more appropriate for this task. The proposed algorithm is inspired by [4] which is originally based on a multi-

dimensional Vandermonde-type decomposition and is applied to multidimensional harmonic retrieval.

The performance of the LVMUSIC and the Tensor MUSIC (TMUSIC) algorithms are compared in numerical simulations for different configurations. This comparison is based on numerical Mean Squared Error (MSE) of all parameters. Moreover the results of MUSIC pseudo-spectra and the numerical Mean Squared Error (MSE) of the DOA estimation for two close sources are also presented.

The following convention is adopted: scalars are denoted as italic letters, vectors as lower-case bold-face letters, matrices as bold-face capitals, and tensors are written as bold-face calligraphic letters. We use the superscripts ^{H}, for Hermitian transposition, * for complex conjugation and $||.||$, the euclidean norm. The mathematical expectation is denoted by $E[.]$ and the Kronecker product is denoted by $\otimes$.

2. SOME MULTILINEAR ALGEBRA TOOLS

This section contains the main multilinear algebra tools used in this paper. Let $\mathcal{A}$, $\mathcal{B} \in \mathbb{C}^{I_1 \times I_2 \times I_3 \times I_4}$, be two 4-dimensional tensors and let $a_{i_1 i_2 i_3 i_4}$, $b_{i_1 i_2 i_3 i_4}$ be their elements. The following operators are required for this paper; for more details, especially the case of n-order tensors, we refer the reader to [6, 7].

2.1. Unfolding

Let us denote $[\mathcal{A}]_n$, $n = 1, \ldots, 4$, the operator which transforms the tensor $\mathcal{A}$ into a matrix by concatenating the different slices of the tensor along the nth mode. For example, $[\mathcal{A}]_1 \in \mathbb{C}^{I_1 \times I_2 I_3 I_4}$.

2.2. Products

- Scalar product of two tensors:
  $< \mathcal{A}, \mathcal{B} >= \sum_{i_1} \sum_{i_2} \sum_{i_3} \sum_{i_4} b^*_{i_1 i_2 i_3 i_4} a_{i_1 i_2 i_3 i_4}$.
- From the scalar product, we define the Frobenius-norm:
  $||\mathcal{A}|| = \sqrt{< \mathcal{A}, \mathcal{A} >}$
- The n-mode product ($n = 1, \ldots, 4$) multiply a tensor by a matrix along the n-th mode. For example, for $n = 2$ and for a matrix $\mathbf{E} \in \mathbb{C}^{J_2 \times I_2}$:
  $(\mathcal{A} \times_2 \mathbf{E})_{i_1 j_2 i_3 i_4} = \sum_{i_2} a_{i_1 i_2 i_3 i_4} e_{j_2 i_2}$.
- Outer product of two tensors: $\mathcal{E} = \mathcal{A} \circ \mathcal{B}$ $\in \mathbb{C}^{I_1 \times I_2 \times I_3 \times I_4 \times I_1 \times I_2 \times I_3 \times I_4}$ with $e_{i_1 i_2 i_3 i_4 j_1 j_2 j_3 j_4} = a_{i_1 i_2 i_3 i_4} . b_{j_1 j_2 j_3 j_4}$.For example, for two vectors, $\mathbf{a}, \mathbf{b}$, their outer product $\mathbf{a} \circ \mathbf{b}$ is a rank-1 matrix.

2.3. Higher Order Singular Value Decomposition

The Higher Order Singular Value Decomposition (HOSVD) decomposes a 4-order tensor $\mathcal{A}$ as follows

$$\mathcal{A} = \mathcal{K} \times_1 \mathbf{U}^{(1)} \times_2 \mathbf{U}^{(2)} \times_3 \mathbf{U}^{(3)} \times_4 \mathbf{U}^{(4)} \quad (1)$$

where $\forall n = 1 \ldots 4$, $\mathbf{U}^{(n)} \in \mathbb{C}^{I_n \times I_n}$ is an orthonormal matrix and where $\mathcal{K} \in \mathbb{C}^{I_1 \times I_2 \times I_3 \times I_4}$ is the core tensor, which satisfies the all-orthogonality conditions [7]. The matrix $\mathbf{U}^{(n)}$ is given by the SVD of the n-dimension unfolding tensor, $[\mathcal{A}]_n = \mathbf{U}^{(n)} \mathbf{\Sigma}^{(n)} \mathbf{V}^{(n)H}$.

Furthermore, if $\mathcal{A}$ is an Hermitian tensor, i.e. $I_1 = I_3$, $I_2 = I_4$ and $a_{i_1,i_2,i_3,i_4} = a^*_{i_3,i_4,i_1,i_2}$, $\forall i_1, i_2, i_3, i_4$, the HOSVD of $\mathcal{A}$ is written [3]:

$$\mathcal{A} = \mathcal{K} \times_1 \mathbf{U}^{(1)} \times_2 \mathbf{U}^{(2)} \times_3 \mathbf{U}^{(1)*} \times_4 \mathbf{U}^{(2)*}. \quad (2)$$

3. POLARIZED SOURCE AND OBSERVATION MODELS

3.1. Polarized source model

Let us consider a linear uniform antenna array of M sensors which can receive N_c polarimetric channels and a polarized source impinging on the array. The one-dimensional DOA of the source is denoted by θ. The signal propagation along the spatial dimension of a polarimetric channel is modelled as follows:

$$\mathbf{d}(\theta) = (1, e^{-2i\pi \frac{d}{\lambda} sin(\theta)}, \ldots, e^{-2i\pi(M-1)\frac{d}{\lambda} sin(\theta)})^T, \quad (3)$$

where d is the distance between two sensors and λ the wavelength. On one sensor, we model the signal received in channel n_c by multiplying its amplitude by ρ_c and shifting its phase by φ_c relative to the first channel (channel 0) as in many polarimetry applications[1]. Thus, for a single sensor, the signal behaviour along the polarization dimension can be modelled as [2]:

$$\mathbf{p}(\boldsymbol{\rho}, \boldsymbol{\varphi}) = (1, \rho_1 e^{i\varphi_1}, \ldots, \rho_{N_c-1} e^{i\varphi_{N_c-1}})^T \quad (4)$$

where $\boldsymbol{\rho} = (\rho_1, \ldots, \rho_{N_c-1})$ and $\boldsymbol{\varphi} = (\varphi_1, \ldots, \varphi_{N_c-1})$ are the gain and the phase shift between channels. Combining equations (3) and (4), the signal propagation along the whole array can be modeled by steering vector $\mathbf{a}(\theta, \boldsymbol{\rho}, \boldsymbol{\varphi}) \in \mathbb{C}^{MN_c}$:

$$\mathbf{a}(\theta, \boldsymbol{\rho}, \boldsymbol{\varphi}) = \mathbf{d}(\theta) \otimes \mathbf{p}(\boldsymbol{\rho}, \boldsymbol{\varphi}). \quad (5)$$

This steering vector is used in this given form for the vectorial approach. However, equations (3) and (4) can also be combined in order to obtain a steering matrix, $\mathbf{A}(\theta, \boldsymbol{\rho}, \boldsymbol{\varphi}) \in \mathbb{C}^{M \times N_c}$, defined as

$$\mathbf{A}(\theta, \boldsymbol{\rho}, \boldsymbol{\varphi}) = \mathbf{d}(\theta) \circ \mathbf{p}(\boldsymbol{\rho}, \boldsymbol{\varphi}). \quad (6)$$

This model keeps the two-dimensional structure of the source and will be used for deriving the proposed tensor MUSIC algorithm.

3.2. Observation model

Let us now consider P independent zero-mean Gaussian sources with unit variance. We assume that K snapshots of the sources impinging the array are available.

[1]For example in polarimetric RADAR, 2 different polarized signals are emitted in HH and VV. These signals are received in 4 polarizations: HH, VV, HV, VH.

Vector model The k-th snapshot, denoted $\mathbf{x}(k) \in \mathbb{C}^{MN_c}$ is modelled by

$$\mathbf{x}(k) = \sum_{p=1}^{P} s_p(k)\mathbf{a}_p(\theta_p, \boldsymbol{\rho}_p, \boldsymbol{\varphi}_p) + \mathbf{b}(k) \tag{7}$$

where $\mathbf{a}_p(\theta_p, \boldsymbol{\rho}_p, \boldsymbol{\varphi}_p)$ is the steering vector of the p-th source and $s_p(k)$ the zero-mean Gaussian-distributed random amplitude of the p-th source. $\mathbf{b}(k)$, is a complex zero-mean Gaussian white noise with covariance matrix $\sigma^2\mathbf{I}_{MN_c}$. Let us denote by $\mathbf{R} = E[\mathbf{x}\mathbf{x}^H]$, the covariance matrix of the data. As $\mathbf{R}$ is unknown in practice, it will be estimated by the Sample Covariance Matrix, $\hat{\mathbf{R}} = \frac{1}{K}\sum_{k=1}^{K} \mathbf{x}(k)\mathbf{x}^H(k)$.

Matrix model For the matrix observation model, the k-th snapshot, denoted $\mathbf{X}(k) \in \mathbb{C}^{M \times N_c}$ is modelled by

$$\mathbf{X}(k) = \sum_{p=1}^{P} s_p(k)\mathbf{A}_p(\theta_p, \boldsymbol{\rho}_p, \boldsymbol{\varphi}_p) + \mathbf{B}(k) \tag{8}$$

where $\mathbf{A}_p(\theta_p, \boldsymbol{\rho}_p, \boldsymbol{\varphi}_p)$ is the steering matrix of the p-th source, $s_p(k)$ the zero-mean Gaussian-distributed random amplitude of the p-th source. $\mathbf{B}(k)$ is a complex Gaussian matrix. Let us denote $\boldsymbol{\mathcal{R}} = E[\mathbf{X} \circ \mathbf{X}^*]$, the covariance tensor defined in [2]. Similarly with the vector approach $\boldsymbol{\mathcal{R}}$ is unknown in practice, it will be estimated by the Sample Covariance Tensor, $\hat{\boldsymbol{\mathcal{R}}} = \frac{1}{K}\sum_{k=1}^{K} \mathbf{X}(k) \circ \mathbf{X}(k)^*$.

4. MUSIC ALGORITHMS

4.1. Vector case

The vector MUSIC algorithm is performed in 3 steps. First the SVD of $\hat{\mathbf{R}}$ is computed

$$\hat{\mathbf{R}} = \hat{\mathbf{U}}\hat{\boldsymbol{\Sigma}}\hat{\mathbf{U}}^H. \tag{9}$$

Then, $\hat{\mathbf{U}}$ is truncated into $\hat{\mathbf{U}}_0$, keeping the $(MN_c - P)$ last columns of $\hat{\mathbf{U}}$ corresponding to the $MNc - P$ eigenvalues. Thus, the columns of $\hat{\mathbf{U}}_0$ represent an orthonormal basis of the estimated noise subspace. Finally, the parameters of the sources are obtained by maximizing the following criterion:

$$\{\theta_p, \boldsymbol{\rho}_p, \boldsymbol{\varphi}_p\} = arg \max_{(\theta, \boldsymbol{\rho}, \boldsymbol{\varphi})} (H_v(\theta, \boldsymbol{\rho}, \boldsymbol{\varphi})) \tag{10}$$

where

$$H_v(\theta, \boldsymbol{\rho}, \boldsymbol{\varphi}) = \frac{1}{||\hat{\mathbf{U}}_0^H \mathbf{a}(\theta, \boldsymbol{\rho}, \boldsymbol{\varphi})||}. \tag{11}$$

4.2. Tensorial case

By analogy with the vectorial case, the tensor MUSIC algorithm is derived as follows. First $\hat{\boldsymbol{\mathcal{R}}}$ is decomposed using the HOSVD procedure as:

$$\hat{\boldsymbol{\mathcal{R}}} = \hat{\boldsymbol{\mathcal{K}}} \times_1 \hat{\mathbf{U}}^{(1)} \times_2 \hat{\mathbf{U}}^{(2)} \times_3 \hat{\mathbf{U}}^{(1)*} \times_4 \hat{\mathbf{U}}^{(2)*}. \tag{12}$$

Then $\hat{\mathbf{U}}^{(1)}$ is truncated into $\hat{\mathbf{U}}_0^{(1)}$ and $\hat{\mathbf{U}}^{(2)}$ to $\hat{\mathbf{U}}_0^{(2)}$ keeping[2] the $(M - r_1)$ last columns of $\hat{\mathbf{U}}^{(1)}$ and respectively the $(N_c - r_2)$ last columns of $\hat{\mathbf{U}}^{(2)}$. The truncation is a correct approximation in most cases, but sometimes the use of an alternating least squares algorithm is necessary for an optimal result [13]. By contrast with the vector algorithm, different truncation ranks can be chosen for the two modes. Finally the parameters of the sources are obtained by maximizing the following criterion:

$$\{\theta_p, \boldsymbol{\rho}_p, \boldsymbol{\varphi}_p\} = arg \max_{(\theta, \boldsymbol{\rho}, \boldsymbol{\varphi})} (H_T(\theta, \boldsymbol{\rho}, \boldsymbol{\varphi})) \tag{13}$$

where

$$H_T(\theta, \boldsymbol{\rho}, \boldsymbol{\varphi}) = \frac{1}{||\mathbf{A}(\theta, \boldsymbol{\rho}, \boldsymbol{\varphi}) \times_1 \hat{\mathbf{U}}_0^{(1)}\hat{\mathbf{U}}_0^{(1)H} \times_2 \hat{\mathbf{U}}_0^{(2)}\hat{\mathbf{U}}_0^{(2)H}||}. \tag{14}$$

5. SIMULATIONS

5.1. Parameters

Numerical simulations are performed for an array of $M = 10$ sensors which receive in $N_c = 3$ polarimetric channels. The number of parameters to be estimated is then equal to five. Let us consider $P = 1$ or $P = 2$ zero-mean, uncorrelated far-field sources located at $\theta_1 = 3°$ and $\theta_2 = -3°$. The polarimetric properties of the second source are the same for all simulations: $\boldsymbol{\rho}_1 = (1, 1, 1)^T$, $\boldsymbol{\varphi}_1 = (0, 0, 0)^T$. For the first source, we consider 2 cases:

- in the first case, $\boldsymbol{\rho}_1 = (1, 1.2, 1.4)^T$, $\boldsymbol{\varphi}_1 = (0, -0.2\ rad, 0.25\ rad)^T$
- in the second case, the polarimetric properties are equal to the first source, $\boldsymbol{\rho}_1 = \boldsymbol{\rho}_2$, $\boldsymbol{\varphi}_1 = \boldsymbol{\varphi}_2$.

$\hat{\boldsymbol{\mathcal{R}}}$ and $\hat{\mathbf{R}}$ are estimated with $K = 200$ snapshots. In order to compute the tensor MUSIC algorithm, the estimates of r_1 and r_2 are required. r_1 corresponds to the spatial dimension. It is straightforward that r_1 is equal to P, the number of sources. Concerning r_2, we consider and analyse both cases $r_2 = 1$ and $r_2 = 2$. An exhaustive study of the rank r_2 will be proposed in a forthcoming paper and especially the link between r_2 and the polarimetric properties of the sources.

5.2. Results

In this section, we will compare the performance of TMUSIC and LVMUSIC (developped in [2]). First, the algorithms are computed for 1 source located at $\theta_1 = 3°$ with $\boldsymbol{\rho} = (1, 1.2, 1.4)^T$ and $\boldsymbol{\varphi} = (0, -0.2\ rad, 0.25\ rad)^T$. The five parameters are estimated. The Mean Squared Error (MSE) of each one is calculated from 100 realizations w.r.t. several values of Signal to Noise Ratio (SNR). The low number of

[2] r_1 and r_2 are the number of important values in the SVD decomposition of $[\hat{\boldsymbol{\mathcal{R}}}]_1$ and $[\hat{\boldsymbol{\mathcal{R}}}]_2$. Their values will be studied in the next section.

realisations is due to the important amount of computational data necessary to estimate the all five parameters. The mean of the five MSE is presented in figure 1. The simulations show that in this case TMUSIC outperforms LVMUSIC.

Therefore, due to the difficulties to obtain results with enough realisations for the five parameters, we now focus on the DOA estimation. We assume that $\boldsymbol{\rho}_1$, $\boldsymbol{\rho}_2$, $\boldsymbol{\varphi}_1$, $\boldsymbol{\varphi}_2$ are known. Moreover the two algorithms are also compared to the classic vector MUSIC without polarization (equivalent to $N_c = 1$) which is denoted VMUSIC. The 3 criteria are computed for 10 realizations with SNR equal to $-6dB$ and for the case where the polarization of the sources are different. Figure 2 shows the 10 pseudo-spectra vs the DOA. Due to the value of the SNR, VMUSIC (2a) does not allow, in most cases, to separate the 2 sources. On the contrary, the LVMUSIC (2b) improves significantly the separation between the 2 sources. TMUSIC (2c) and (2d) gives better results than the vector algorithms. The results for $r_2 = 1$ and $r_2 = 2$ are similar.

Then, the accuracy of each algorithms is studied. To this end, the mean of $MSE(\hat{\theta}_1)$ and $MSE(\hat{\theta}_2)$ is computed for 1000 realizations w.r.t. several values of SNR. We can consider that this measure is linked to the resolution of the algorithms. The results obtained are presented in figure 3 from the case $\boldsymbol{\rho_1} \neq \boldsymbol{\rho}_2$, $\boldsymbol{\varphi}_1 \neq \boldsymbol{\varphi}_2$ and figure 4 for the second case where the polarimetric properties are equal. One can see that adding the polarization enhances the resolution of LVMUSIC when the polarimetric properties are different. On the contrary, when the polarimetric properties are equal, the performance of LVMUSIC are almost equal to VMUSIC. Indeed, as the polarization parameters of the two sources are the same, the polarization does not provide additional informations to improve the performance of the LVMUSIC algorithm. By contrast TMUSIC outperforms the other methods for both cases. This can be explained by the fact that the spatial part of TMUSIC may be seen as a vector MUSIC without polarization computed with $K' = N_c K = 3K$ snapshots. The MSE of VMUSIC computed with $K' = 3K$ is presented in figure 3 and 4. We notice that it is very close to the MSE of TMUSIC which confirms this explanation. We also notice that the performance of TMUSIC is almost equal for $r_2 = 1$ or $r_2 = 2$.

6. CONCLUSION

In this paper, we worked on parameters estimation for a simulated mixture of polarized sources. We developed and studied a tensor MUSIC algorithm based on HOSVD of the data covariance tensor, allowing to estimate jointly the DOA and polarimetric parameters of the sources. We computed the numerical performance of this algorithm and we compared it with vector MUSIC algorithms. We showed by numerical simulations that tensor MUSIC outperforms the vectorial approach in the considered scenarios, due to a better use of the multilinear structure of the data.

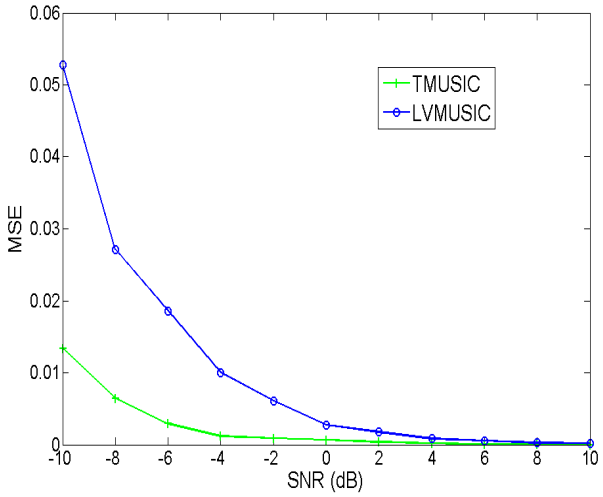

Fig. 1: Mean of MSE of the 5 parameters VS SNR for 1 source located at $\theta_1 = 3°$ with $\boldsymbol{\rho} = (1, 1.2, 1.4)^T$ and $\boldsymbol{\varphi} = (0, -0.2\ rad, 0.25\ rad)^T$

In order to confirm the interest of our approach, it could be interesting to adapt the CP algorithm and the Cramér Rao bound derived in [12] to our model and to compare them. We are also currently working on the theoretical performance of TMUSIC using a perturbation method adapted from [14].

7. REFERENCES

[1] G. Showman, W. Melvin, and M. Belenkii, "Performance evaluation of two polarimetric STAP architectures," in *Proc. of the IEEE Int. Radar Conf.*, 2003, pp. 59–65.

[2] S. Miron, N. Le Bihan, and J. Mars, "Vector-sensor MUSIC for polarized seismic sources localization," *EURASIP Journal on Advances in Signal Processing*, vol. 2005, pp. 74–84, 2005.

[3] M. Haardt, F. Roemer, and G. Del Galdo, "Higher-order SVD-based subspace estimation to improve the parameter estimation accuracy in multidimensionnal harmonic retrieval problems," *IEEE Trans. on Proc. Sig. Proc.*, vol. 56, no. 7, pp. 3198–3213, July 2008.

[4] R. Boyer, "Decoupled root-MUSIC algorithm for multidimensional harmonic retrieval," in *IEEE 9th Workshop on Signal Processing Advances in Wireless Communications*, Recife, Brazil, 2008, pp. 16 – 20.

[5] G. Favier, M.N. da Costa, A.L.F. de Almeida, and J.M.T. Romano, "Tensor space time (TST) coding for MIMO wireless communication systems," *Signal Processing*, vol. 92, pp. 1079 – 1092, April 2012.

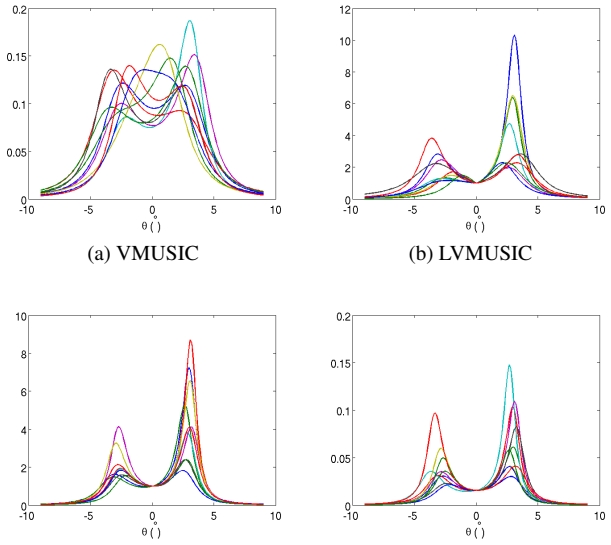

(a) VMUSIC (b) LVMUSIC

(c) TMUSIC with $r_2 = 1$ (d) TMUSIC with $r_2 = 2$

Fig. 2: MUSIC pseudo-spectra between $-9°$ and $9°$ for 10 realizations of the first case of polarization at $SNR = -6dB$ with 2 sources located at $\theta_1 = -3°$ and $\theta_2 = 3°$.

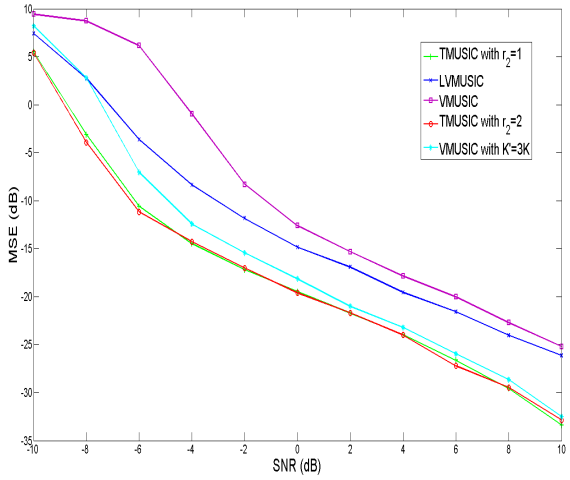

Fig. 3: Mean of MSE(θ_1) and MSE(θ_2) VS SNR for 2 sources located at $\theta_1 = -3°$ and $\theta_2 = 3°$ with different polarimetric properties: $\rho_1 = (1,1,1)^T$, $\varphi_1 = (0,0,0)^T$, $\rho_2 = (1,1.2,1.4)^T$, $\varphi_2 = (0,-0.2\,rad,0.25\,rad)^T$

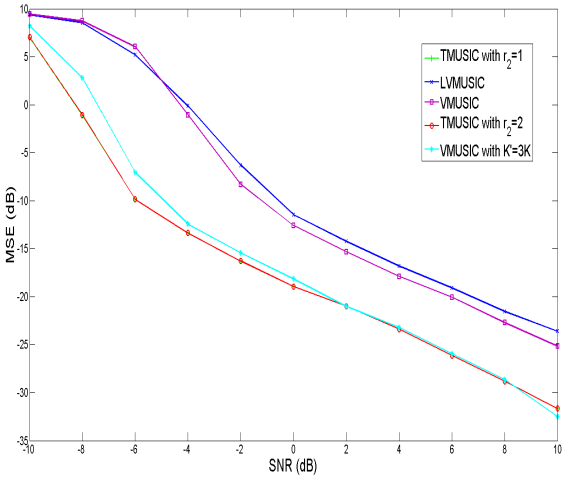

Fig. 4: Mean of MSE(θ_1) and MSE(θ_2) VS SNR for 2 sources located at $\theta_1 = -3°$ and $\theta_2 = 3°$ with the same polarimetric properties.

[6] T. Kolda and B. Bader, "Tensor decompositions and applications," *SIAM Review*, vol. 51, pp. 455 – 500, 2009.

[7] L. De Lathauwer, B. De Moor, and J. Vandewalle, "A multilinear singular value decomposition," *SIAM J. Matrix Anal. Apl.*, vol. 24, no. 4, pp. 1253–1278, 2000.

[8] N.D. Sidiropoulos, R. Bro, and G.B. Giannakis, "Parallel factor analysis in sensor array processing," *IEEE Trans. on Proc. Sig. Proc.*, vol. 48, no. 8, pp. 2377–2388, August 2000.

[9] N.D. Sidiropoulos, R. Bro, and G.B. Giannakis, "Blind PARAFAC receivers for DS-CDMA systems," *IEEE Trans. on Proc. Sig. Proc.*, vol. 48, no. 3, pp. 810–823, March 2000.

[10] R. A. Harshman, "Foundation of the parafac procedure: Model and conditions for an explanatory multi-mode factor analysis," *UCLA Working Papers in Phonetics*, vol. 16, pp. 1–84, December 1970.

[11] X. Gong, Z. Liu, Y. Xu, and M.I. Ahmad, "Direction-of-arrival estimation via twofold mode-projection," *Signal Processing*, vol. 89, pp. 831–842, may 2009.

[12] S. Miron, X. Guo, and D. Brie, "DOA estimation for polarized sources on a vector-sensor array by PARAFAC decomposition of the fourth-order covariance tensor," in *Proceedings of EUSIPCO*, Lausanne, Switzerland, August 2008.

[13] L. De Lathauwer, B. De Moor, and J. Vandewalle, "On the best rank-1 and rank-$(r_1, r_2, ..., r_n)$ approximation and applications of higher-order tensors," *SIAM J. Matrix Anal. Apl.*, vol. 21, no. 4, pp. 1324–1342, 2000.

[14] H. Krim, P. Forster, and J.G. Proakis, "Operator approach to performance analysis of root-music and root-min-norm," *IEEE Trans. on Sig. Proc.*, vol. 40, no. 7, pp. 1687 – 1696, July 1992.